

THE FINE STRUCTURE OF ASTROCYTES IN THE CEREBRAL CORTEX AND THEIR RESPONSE TO FOCAL INJURY PRODUCED BY HEAVY IONIZING PARTICLES

DAVID S. MAXWELL, Ph.D., and LAWRENCE KRUGER, Ph.D.

From the Department of Anatomy and Brain Research Institute, University of California at Los Angeles, and Veterans Administration Hospital, Long Beach, California

ABSTRACT

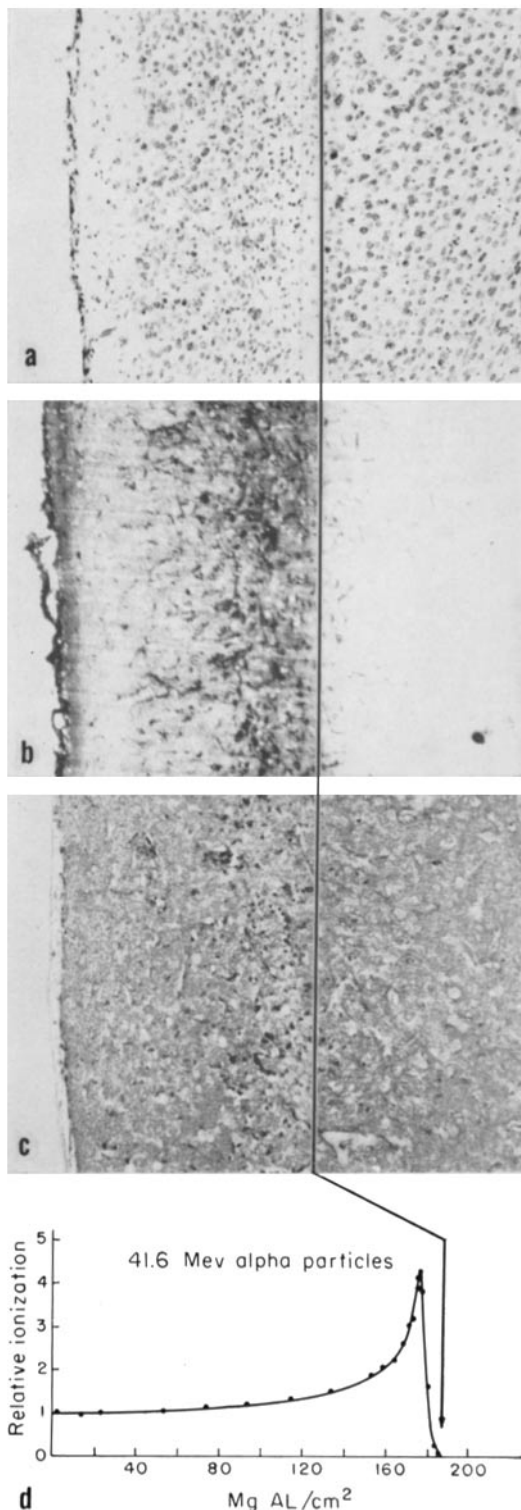
Normal and reactive astrocytes in the cerebral cortex of the rat have been studied with the electron microscope following focal alpha particle irradiation. The presence of glycogen and approximately 60-A fibrils identify astrocyte cytoplasm in formalin-perfused tissue. The glycogen particles facilitate the identification of small processes and subpial and perivascular end-feet. Both protoplasmic and fibrous astrocytes contain cytoplasmic fibrils and should be distinguished on the basis of the configuration of their processes and their distribution. Acutely reactive astrocytes are characterized by a marked increase in the number of glycogen granules and mitochondria from the first day after irradiation. These cells later hypertrophy and accumulate lipid bodies and increased numbers of cytoplasmic fibrils. The glial "scar" consists of a greatly expanded volume of astrocyte cytoplasm filled with fibrils and displays no signs of astrocyte death, reversion to primitive forms, or extensive multiplication.

INTRODUCTION

The characteristics of the neuroglial elements of the central nervous system have been defined primarily by nuclear stains or by heavy metal impregnation of glial cytoplasm (5). Of these elements, the most easily recognized is the astrocyte. With the introduction of modern electron microscopy it has been possible to study the fine structure of astrocytes and to identify some of the cytoplasmic inclusions seen under light microscopy, but some disagreement has remained concerning the identity of astrocytes (1, 3, 4, 6, 7, 8, 10, 11, 16, 17, 19, 22, 23, 24, 28, 29, 33, 34).

The present report deals with the characteristics of astrocytes in formalin-perfused tissue from the cerebral cortex of the rat, and describes the unique

transformations which occur in these elements in response to injury. The experimental material chosen was a narrow laminar lesion of the cerebral cortex produced by a monoenergetic beam of fast alpha particles (18). Use of laminar lesions thus produced offers the advantage of permitting study of both normal and irradiated cells in the same thin sections in the electron microscope, and, additionally, provides degenerative changes of neural elements not accompanied by gliosis and vascular disruption. Evidence will be presented from this material to show that the astrocyte is a distinctive element which can be readily distinguished from other glial cells. In addition, it will be shown that an examination of the organelles of astrocytes



reveals a sequence of pathological changes which characterize the reactive astrocyte of classical microscopy. Preliminary reports of some aspects of this work have been presented (19, 20).

METHODS

The material presented in this report is limited to selected portions of a larger study on the morphological aspects of lesions in the cerebral cortex produced with ionizing radiation. All the material presented here was obtained from female rats 28 to 30 days old at the time of irradiation. The normal tissue was obtained from the normal hemisphere of these same animals and from untreated animals.

Experimental lesions were produced with a monoenergetic beam of alpha particles in a manner described in detail by Malis *et al.* (18) for similar procedures. Because of the special character of this method for experimental destruction, a brief explanatory comment on those features relevant to this study and on special technical methods used here is included. A more complete description can be found elsewhere (2, 18). The essential features can be best understood in terms of the distribution of energy in the cortex, which is described by the energy release curve shown in Fig. 1 *d*. The shape of this curve and the range of particles is determined by the particle velocity and the density of the medium to be

FIGURE 1 a. Laminar lesion in the cerebral cortex indicated by the absence of neurons and a slight increase in number of glial nuclei. Forty-three days after irradiation. Tissue irradiated with alpha particles, 6000 rad (surface dose). Thionin stain. $\times 90$. A line which indicates the end of range of particles constitutes the lower limit of the lesion *a*, *b*, and *c*, and corresponds to the position of the arrow in *d*.

b. Silver impregnation of reactive astrocytes in the irradiated portion of the cortex in the same animal as in *a*. Modified Bielschowsky stain. $\times 90$.

c. Periodic acid-Schiff (PAS) preparation of a heavy dose laminar lesion (20,000 rad, surface dose) 2 days after irradiation. The rapid accumulation of the PAS-positive material is associated with the zone of astrocytic reaction. $\times 90$.

d. Energy release curve (Bragg curve) for particles used in this study, showing relative ionization (or energy release) registered in a saturated ionization chamber after passage through aluminum foils of varying thickness. The peak of this curve is responsible for producing the laminar lesion at those doses which do not produce destruction with a surface dose. Only the cortex from the surface to the end of the particle range (arrow) is bombarded by heavy ionizing particles.

penetrated. The unique advantages of this method are that (a) energy release is maximal near the end of particle range (the Bragg effect), so that with appropriate choice of dose one can destroy a layer in the middle of the cortex with minimal damage to overlying layers, and (b) the spatial decay of this peak of destruction is approximately 10μ for a medium the density of tissue in the present experimental arrangement, and, consequently, neurons remain intact 10 to 20μ below the zone in which all neurons are destroyed (Fig. 1 a).

The precisely delimited edge is particularly advantageous for electron microscopy, in providing material in which the lesion area can be compared with essentially normal tissue in the same block and frequently within the same grid square. However, it should be noted that the entire cortex above the region of maximal ionization or aneuronal zone¹ (subsequently to be referred to as "lesion zone") also receives a significant dose of radiation, and it is clear that lesser but real changes are produced above the lesion zone.

The lesion zone is readily identified in Nissl-stained preparations (Fig. 1 a) by the complete absence of neuron perikarya, leaving a band containing only glial nuclei whose numbers are only slightly increased after mild or moderate irradiation doses. In some cases it has also been possible to impregnate cells selectively with silver throughout the laminar lesion and less extensively in the region above the lesion, which receives a lesser dose, corresponding to the left side of the Bragg curve (Fig. 1 d). These cells are presumably reactive astrocytes, as judged by their size and processes in modified Bielschowsky preparations (Fig. 1 b). It is also possible with high doses to show a relatively prompt, acute accumulation of PAS-positive material in the lesion zone (Fig. 1 c), although with lower doses a less synchronized prolonged response of astrocytes results in less distinct cytoplasmic accumulations and it is usually difficult to identify the exact distribution of PAS-positive material. The identification of this material as glycogen by enzymatic digestion and its distribution in astrocyte cytoplasm has been described in detail by Klatzo *et al.* (13).

All lesions were produced with 41.6-Mev alpha particles (10.4 Mev per nucleon) obtained from the Heavy Ion Linear Accelerator at the Lawrence Radiation Laboratory of the University of California, Berkeley. Dosages in this paper refer to the surface dose or energy at the left side of the curve in Fig. 1. The peak dose is several times higher and can be

¹The permanent loss of neurons in the lesion refers only to perikarya. Although neuronal processes are also injured, some normal dendrites, axons, and terminals can be identified in the lesion zone at all stages studied (20).

obtained approximately by multiplying the surface dose by the ratio of the peak to surface value in this curve. These values can easily be converted to more conventional physical units such as number of ions or ergs per gram or square centimeter by simple calculations discussed in detail elsewhere (18).

All lesions were made within a portion of layer II, III, or IV of the right striate field of rat cerebral cortex by positioning a lead shield 1 mm thick with a circular aperture 7.2 mm in diameter over the bone overlying this part of the brain. The animals were anesthetized, the skin was opened, and the head and body were rigidly fixed on a board to which the shield could be attached. After the shield was positioned, the board was mounted on a rack and pinion device for aligning the aperture against the outer aluminum foil of an ionization chamber (used for measurement of dose) mounted on the end of a long beam pipe emerging from one of the accelerator ports. An integrator was adjusted to stop the beam automatically after the appropriate number of particles was delivered to the brain. The skin was then closed and the animals were allowed to recover. The cranial cavity was never opened before the sacrifice date.

The ionization chamber used for measuring beam current and the deflector plates for integration of particle count were calibrated against a solid state particle detector which in turn was calibrated against a polonium alpha source and a Faraday cup. The ionization chamber was sufficiently saturated to provide linear readings within the range of beam currents employed. Calibrations and exposure of photographic plates for checking homogeneity of beam cross-section were performed before, in the middle of, and at the end of the complete experimental run. An uncorrected error in determining dose is introduced by failure to correct for a small energy loss and scatter in air between the foil at the end of the beam pipe and the surface of the brain, and for the increase in density due to the presence of bone. However, these errors should be approximately constant, and scatter was minimized by placing the lead shield against the end of the beam pipe.

Five dosage ranges were studied. These were surface doses of 6000, 9000, 12,000, 20,000, and 30,000 rads.² Doses of 6000 and 9000 rads produced moderate laminar lesions within 2 and 1 weeks, respectively. A heavy laminar lesion was produced with 12,000 rads, and complete destruction to the end of particle range occurred with 20,000 and 30,000 rads. Because of extensive vascular destruction which complicated the interpretation of lesions in the 12,000 to 30,000 rad range within 1 week after irradiation, only changes in the tissue adjacent to the heavy dose lesions will be presented here.

²One rad = 100 erg/gm or 6.25×10^7 Mev/gm.

Animals were sacrificed at 1, 2, 3, 5, 10, 11, 22, 35, 49, 84 days, 5, 6, 8, 9, 10, 12, and 20 months by inducing barbiturate anesthesia before perfusion. In most cases, tissue of satisfactory quality for electron microscopy was obtained from more than one animal for each dose and time. Half of each lesion was taken for light microscopy, and Nissl-stained controls were obtained for all lesions to confirm the depth and severity of each lesion. A PAS stain was obtained for 12 selected lesions. All tissue for conventional microscopy was embedded in paraffin and sectioned at 10 μ , and all sections were mounted and stained.

Animals were perfused through the ascending aorta with a buffered formaldehyde solution prepared according to the method of Pease (25). This method utilizes a 4 per cent formaldehyde solution prepared without the usual methanol preservative and diluted in Millonig's phosphate buffer. The osmium tetroxide postfixation solution is prepared in the same buffer. The principal advantage of formaldehyde as a killing and initial fixing agent is a remarkable uniformity of fixation quality from region to region and from animal to animal in a large series. It may be worth emphasizing that this method appears to provide an opportunity for studying many experimental conditions requiring comparison from one animal or region to the next, that have previously been impossible with procedures of tissue preparation which leave spotty areas of poor fixation. On the other hand, it must be borne in mind that artifacts resulting from faulty perfusion or excessive perfusion pressures are possible, although they seem to be readily recognizable. The buffered formaldehyde mixture used in this study appears to be somewhat hypertonic, and therefore data obtained with respect to water and electrolyte distribution or the state of hydration of astrocyte cytoplasm must be interpreted with great caution.

After perfusion, the calvarium was quickly removed and a portion of hemisphere containing one-half of the lesion was removed for study by light microscopic methods. The remainder of the lesion was usually cut into strips 1 mm or less in width, and 1 mm or more in depth. These were quickly transferred to buffered osmium tetroxide for 1 to 2 hours. The tissue was dehydrated, trimmed if neces-

sary, and then embedded in Araldite or Epon after the method of Luft (15). For our purposes, Araldite was generally found to be most satisfactory. Initially, several animals at each dose and interval were sacrificed for embedding in Araldite and Epon; later in the study all tissue was embedded in Araldite.

Some thin sections were mounted on Formvar films over slotted grids, to facilitate localization of the lesion areas. Once the lesion was identified, however, further study was carried out on unsupported sections. All electron micrographs in this report were prepared from sections of Araldite-embedded material. Thin sections were stained with lead hydroxide (35) or lead citrate (27) and photographed in the RCA EMU 3E or the Hitachi HU 11A electron microscope.

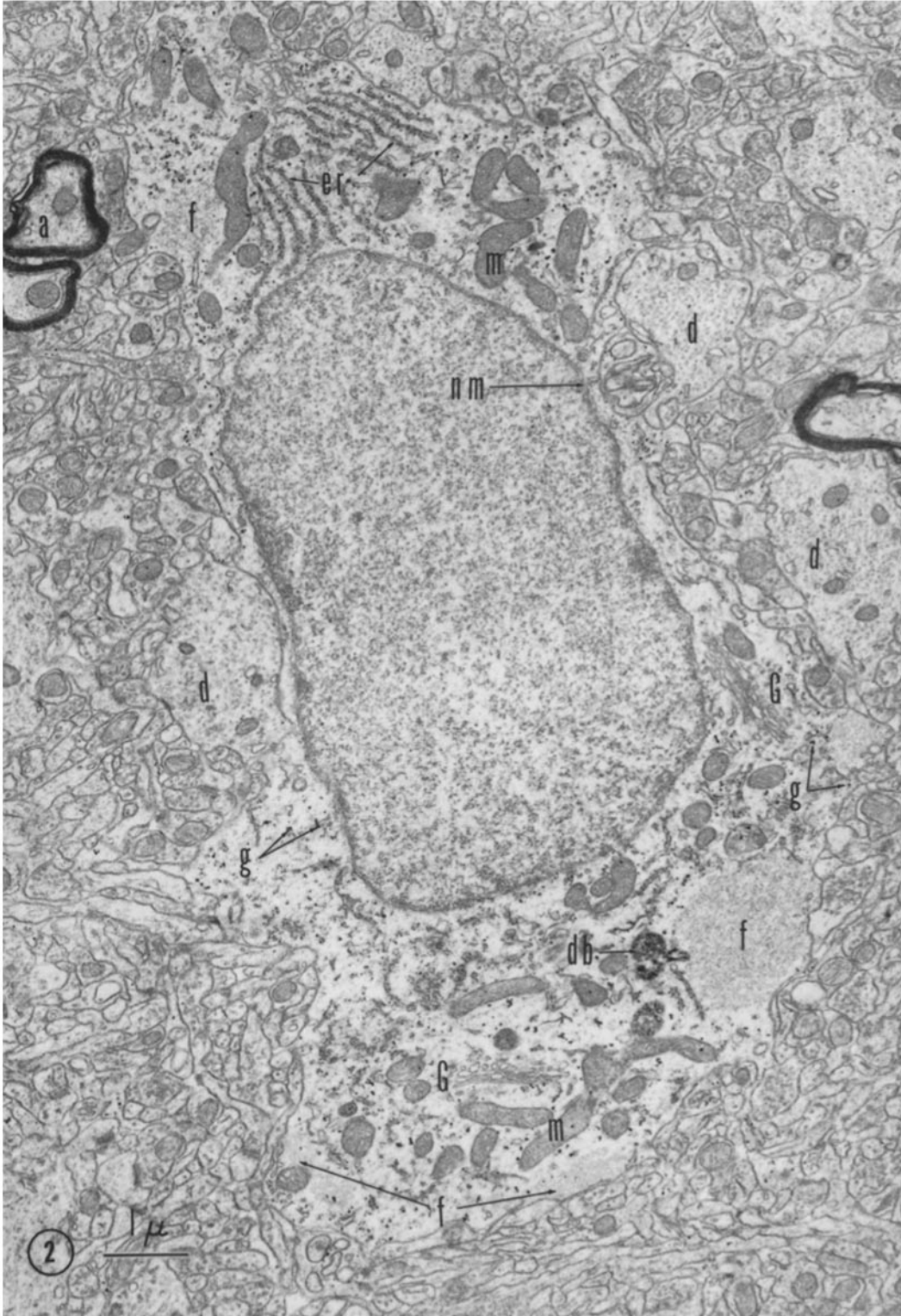
RESULTS

Normal Astrocytes

The astrocyte, as studied with the electron microscope, is a distinctive cellular component of the mammalian central nervous system. In the cerebral cortex of the rat, astrocytes provide the most abundant cytoplasm applied to the walls of small blood vessels, and a layer immediately subjacent to the pia. The cell body contains an irregularly round or oval nucleus, and the cytoplasm around the nucleus is abundant but contains relatively few electron-opaque components, so that the over-all effect is of a rather "watery" composition. In the cerebral cortex, the freely branching character of its processes is diagnostic of the protoplasmic astrocyte of light microscopy. As seen in electron microscopic as well as light microscopic examination, the astrocyte is the largest glial cell encountered in the cortex.

Accumulations of cytoplasmic fibrils can be identified in the perinuclear cytoplasm, and in the larger processes of astrocytes (Figs. 2, 3, and 4). The fibrils are gathered into small wisps and/or into bundles as large as 1 to 2 μ in diameter. The individual fibrils are strands about 60 A in di-

FIGURE 2 Protoplasmic astrocyte, normal cerebral cortex. The nucleus occupies the center of the field, and the nuclear membrane is indicated (*nm*). The endoplasmic reticulum near the top (*er*) is well organized. Clusters of Golgi membranes (*G*) are characteristic of astrocytes, as are the mitochondria (*m*) with dense matrix. A granular dense body (*db*) is indicated in the cytoplasm. Bundles of fibrils (*f*) are scattered through the perinuclear cytoplasm. These fibrils are much finer than the filaments characteristic of axons (*a*) or the tubules common in dendrites (*d*). Glycogen granules (*g*) are distributed through the cytoplasm, but at this magnification are difficult to indicate individually.



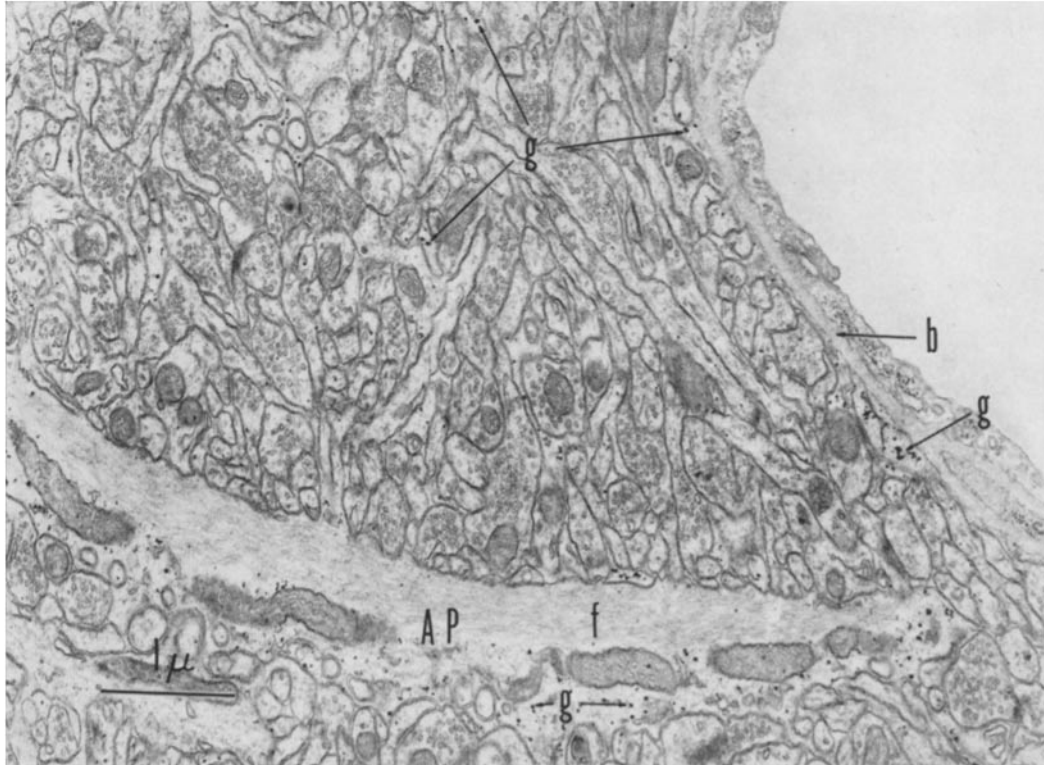


FIGURE 3 Normal cerebral cortex. A part of a capillary is seen in the upper right. The basement membrane of the endothelial lining is indicated (*b*). The presence of glycogen (*g*) characterizes attenuated astrocyte end-feet applied to the basement membrane, and can also be seen in astrocyte processes in the neuropil. A large astrocyte process (*AP*) containing glycogen (*g*) and a bundle of fibrils (*f*) sweeps across the lower part of the figure.

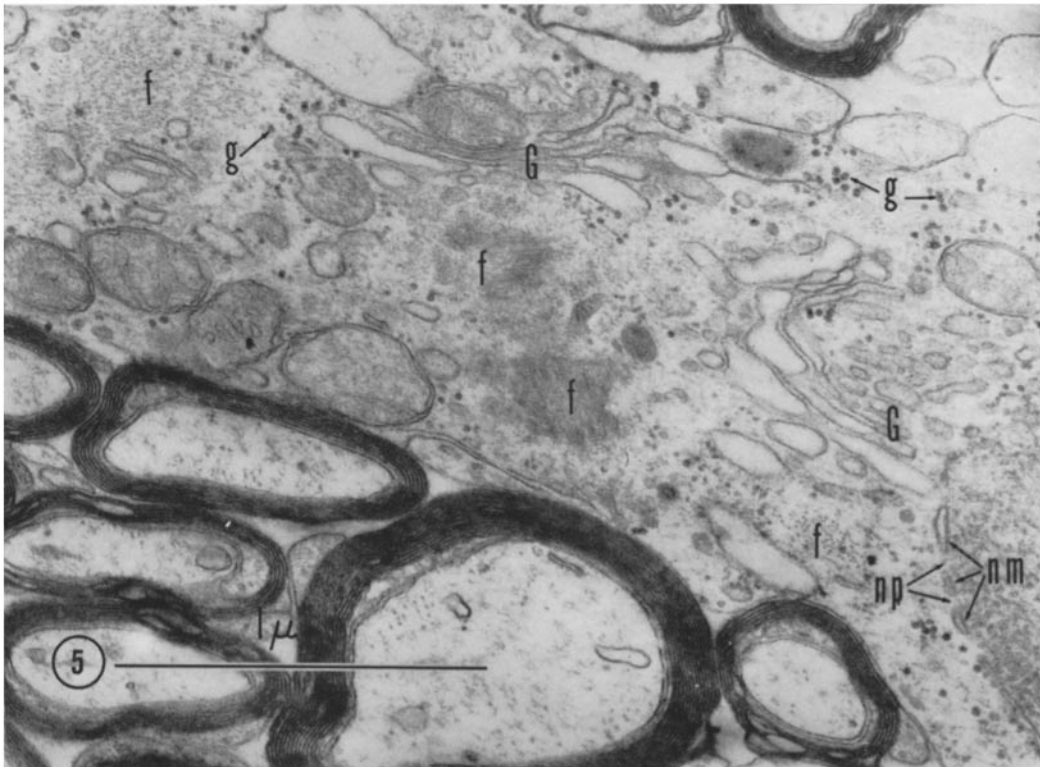
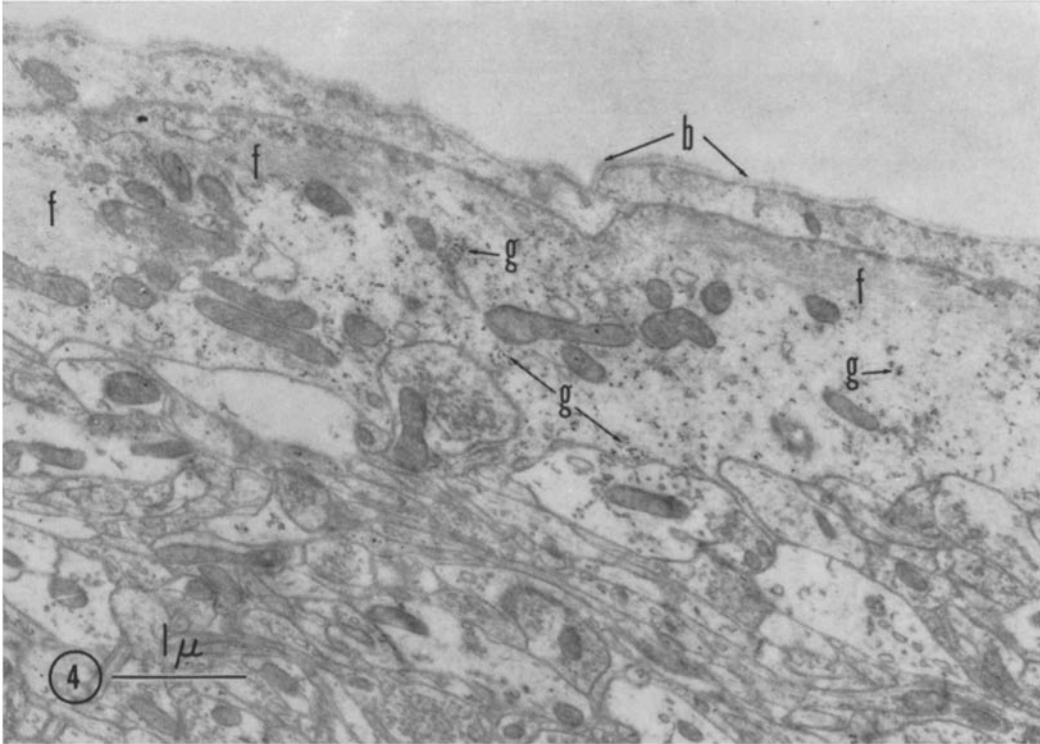
ameter and of indeterminate length. They stain only lightly with lead and uranium salts and phosphotungstic acid. In the perinuclear cytoplasm (Fig. 2) the course of any one bundle or wisp cannot be followed over any appreciable distance, a fact which suggests a sinuous course through the cytoplasm. In the larger processes,

however, they are constrained to a straighter course, and may be followed for considerable distances (Fig. 3). Dense bodies with granular substructure are occasionally encountered (Fig. 2) which conceivably are related to lysosomes.

Unevenly scattered through the cytoplasm are dense granules 150 to 400 Å in diameter. These

FIGURE 4 Subpial astrocyte end-feet, normal cerebral cortex. The basement membrane (*b*) of the pia mater is indicated. The pia has been stripped away during preparation. Two layers of end-feet separate the neuronal elements from the basement membrane in this section. Fibrils (*f*) and glycogen (*g*) are indicated.

FIGURE 5 Fibrous astrocyte, normal subcortical white matter. A portion of the nucleus is seen at the extreme right of the figure. Its nuclear membrane (*nm*) is interrupted by "nuclear pores" (*np*). Prominent cisterns of the Golgi membranes (*G*) are indicated in the perinuclear cytoplasm. The cytoplasm is characterized by glycogen granules (*g*), and by bundles of fibrils (*f*) cut in cross-section in the upper left and lower right, and tangentially in the central part of the figure.



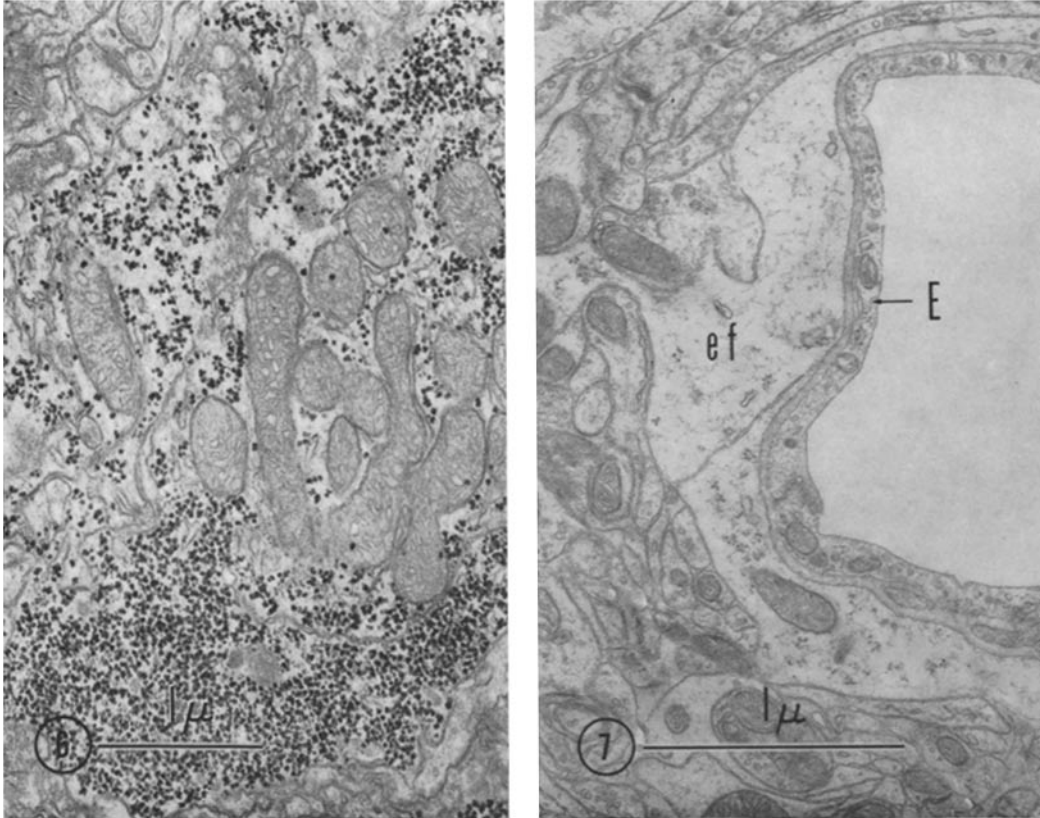


FIGURE 6 One day post irradiation, 6000 rad. The dose indicated in this and succeeding figures is expressed as the surface dose of alpha particles. Typical early acute reactive astrocyte cytoplasm, filled with glycogen granules and mitochondria with their characteristic dense matrix.

FIGURE 7 Cerebral cortex, fixed after 3 minutes of arrested circulation. Capillary astrocyte end-feet (*ef*) appear somewhat swollen, and totally devoid of glycogen. The endothelial lining is indicated (*E*).

structures stain more intensely with lead salts than any other cytoplasmic component in the cerebral cortex, and are identified as glycogen particles (26). In the normal astrocyte, these particles are only sparsely scattered through the perinuclear cytoplasm (Fig. 2), but seem somewhat more abundant in the processes and in the vascular end-feet (Fig. 3). They are also evident in subpial end-feet (Fig. 4).

The nucleoplasm of normal astrocytes is finely granular and of only moderate density. It is evenly distributed through the nucleus, except at the rim of the nuclear profile, where it is aggregated into clumps just under the nuclear membrane (Fig. 2). The nucleolus can be recognized as a loosely organized condensation of nuclear granules. The nuclear cleft is commonly dilated into small cisterns and is occasionally found to be

continuous with the endoplasmic reticulum. Nuclear "pores" can also be identified (Fig. 5).

The endoplasmic reticulum is scanty, and may be only modestly organized or simply dispersed in single strands through the perinuclear cytoplasm (Fig. 2). RNP particles ("ribosomes") are aligned in a relatively sparse array along the membranes of the endoplasmic reticulum, and may also be scattered at random through the cytoplasm. The Golgi membranes, on the other hand, generally are organized into stacks of plates and/or tubules several layers thick (Figs. 2 and 5). Several such clusters may be observed in any one profile of the perinuclear cytoplasm. Neither the endoplasmic reticulum nor the Golgi membranes are commonly encountered in smaller processes of astrocytes.

The mitochondria of astrocytes commonly appear to contain a denser matrix material than is

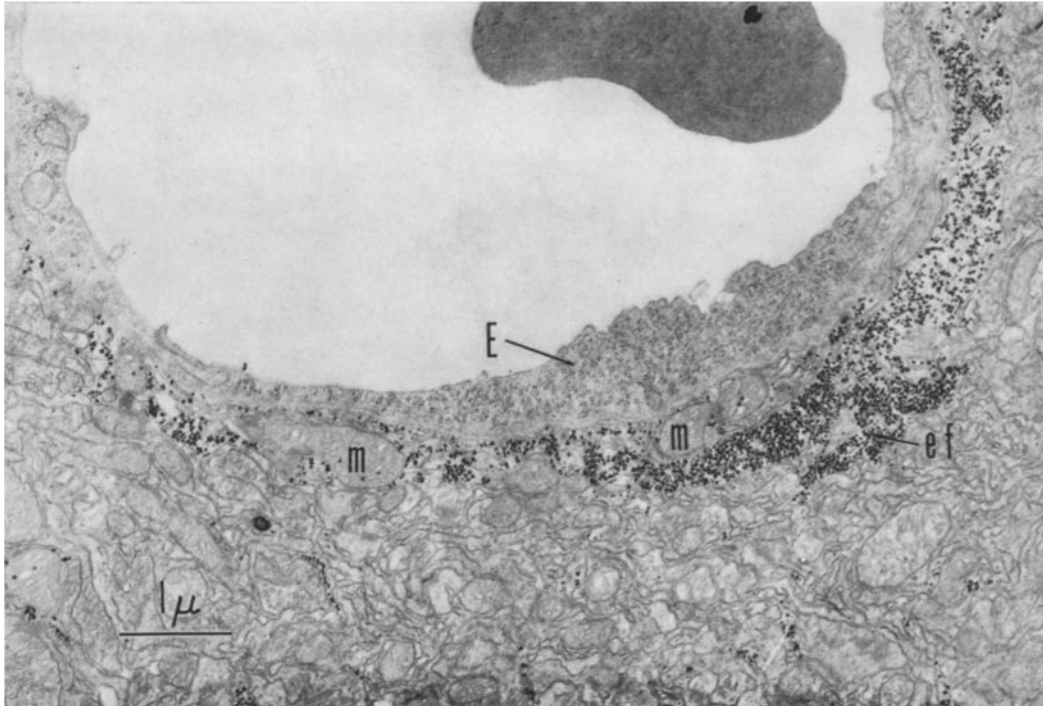


FIGURE 8 One day post irradiation, 6000 rad. The lumen of a blood vessel containing one red cell occupies the upper part of the figure. The endothelial cell lining the capillary is indicated (*E*). Astrocyte end-feet (*ef*) are enlarged, and filled with prominent glycogen granules and numerous mitochondria (*m*).

usually seen in mitochondria of other cortical cells (Fig. 2), but this is not always evident in normal cortex.

Glycogen particles are not found in poorly preserved material, such as that obtained after faulty perfusion, and we have not found them after preservation by immersing fresh tissue in fixative. Presumably, a delay between the circulatory arrest preceding fixation and the actual killing and fixation of the tissue permits consumption of astrocytic glycogen by anaerobic glycolysis. To test this assumption, cortical tissue was prepared from normal animals in the same fashion as described in "Methods," except that the ascending aorta was clamped for 3 minutes after thoracotomy; the clamp was then removed and the perfusion begun. The tissue thus prepared was compared with tissue fixed at the same time according to our customary procedures. Figure 7 illustrates rat cerebral cortex fixed after 3 minutes of circulatory arrest. This material is preserved satisfactorily, except for the astrocyte cytoplasm, which is completely devoid of glycogen particles, and seems to be swollen.

The protoplasmic astrocytes of gray matter (Fig. 2) and the fibrous astrocytes of white matter (Fig. 5) both contain the same complement of organelles, including the prominent glycogen granules throughout the cytoplasm, and cytoplasmic fibrils in the perinuclear cytoplasm and in larger processes. These two types of astrocytes therefore probably belong to the same glial cell category. It has been suggested that the difference between them is simply that of external configuration imposed upon them by the other cellular elements in the environment (29). Thus the processes of the fibrous astrocyte in white matter are generally straight and sparsely branched, because of the presence of numerous myelinated fibers. The protoplasmic astrocyte is found in neuropil, where its profusely and finely branched processes are inserted into the interstices between some of the smallest cortical elements (Fig. 3). Nevertheless, the distinction between fibrous and protoplasmic astrocytes is now so firmly entrenched in classical literature that it must be taken into account in electron microscopy, or at least it must not be distorted. It would be a disservice to future

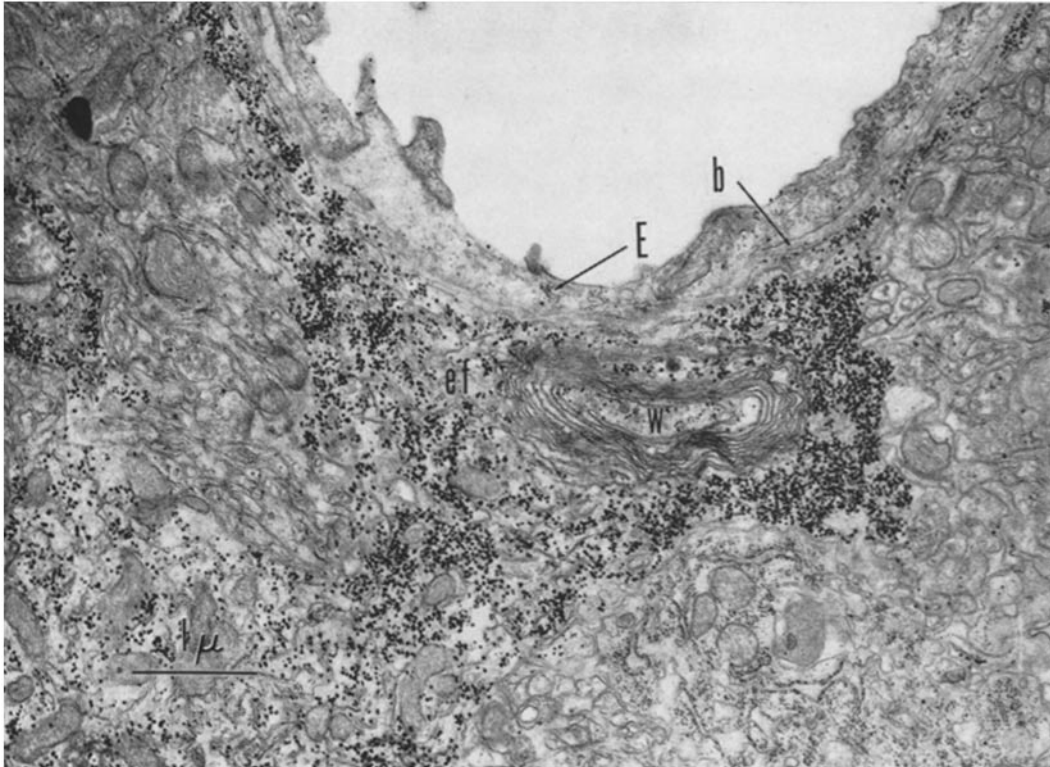


FIGURE 9 Five days post irradiation, 8000 rad. A large glycogen-filled astrocyte end-foot (*ef*) is applied to the basement membrane (*b*) of a small vessel whose endothelial lining is indicated (*E*). A whorl of membrane (*W*) is prominent in the end-foot.

students to fail to account for the correspondence between this tradition of light microscopy and its extensive literature on the one hand, and, on the other, the rapidly developing literature of electron microscopy of neuroglia.

Unfortunately, it has become current vogue to use the presence of cytoplasmic fibrils as the diagnostic feature of astrocyte cytoplasm.³ This criterion is of only limited usefulness (the fibrils

³ The fibrils themselves have led to some confusion in the literature. Although our findings are in best agreement with the report (33) of fine filaments of indeterminate length and about 60 Å in diameter (as determined in micrographs at higher magnification than those shown), some of the discrepancies (1, 8, 10) are undoubtedly due to staining methods and other technical factors. With the methods employed here, cytoplasmic profiles containing filaments 100 to 200 Å in diameter, but consistently devoid of glycogen particles, seem generally to be either axons or dendrites, depending upon the size of the filaments (see Fig. 2).

are rarely found in finer processes of astrocytes, and irregularly in vascular end-feet), and may at times lead to error (rarely, a few wisps of fibrils may be found in the perinuclear cytoplasm of cells which by other criteria should be called oligodendrocytes).

An even more unfortunate custom has grown from this usage, in the tendency to refer to fibril-containing astrocytes as "fibrous astrocytes." This does not conform to the customary definition of the fibrous astrocyte. Furthermore, it forces the designation "protoplasmic astrocyte" out of use, since most astrocytes in the cortex clearly contain cytoplasmic fibrils, although the latter are more prominent in the "fibrous" astrocytes of white matter. The fibrils in question (approximately 60 Å in diameter) are far beyond the limits of resolution of the light microscope. Presumably, since they are regularly gathered into bundles, it is the aggregates of these fibrils which form the basis for light microscope descriptions of glial cytoplasmic fibers.

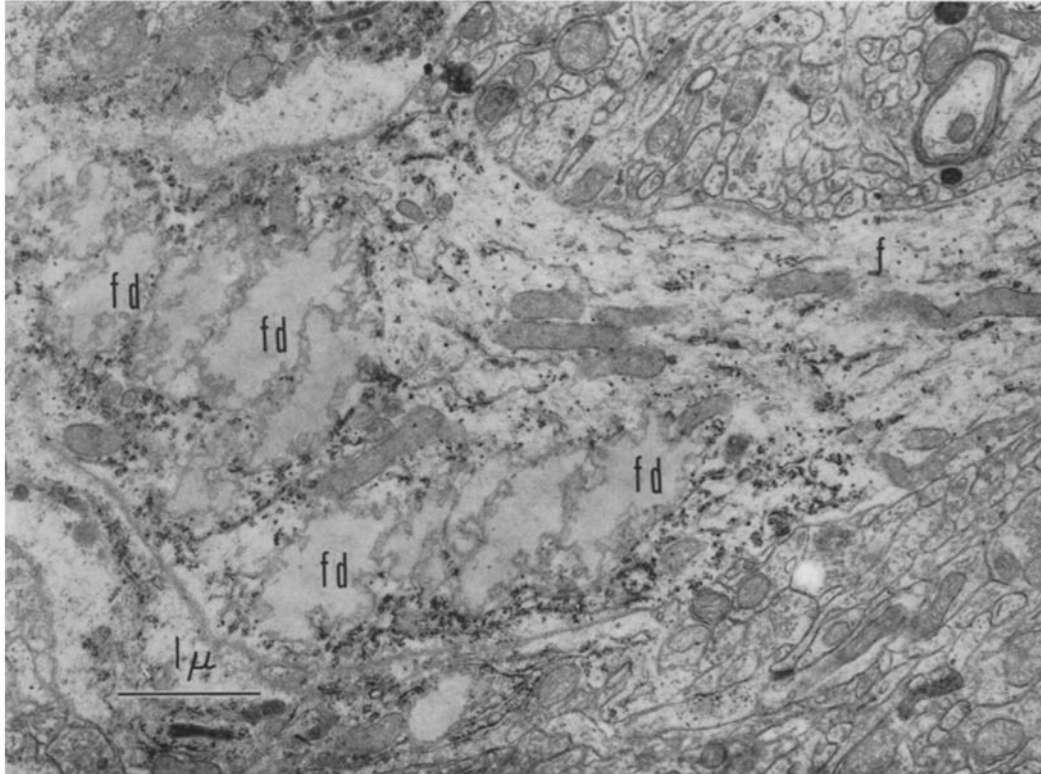


FIGURE 10 Eleven days post irradiation, 9000 rad. Astrocyte cytoplasm, containing several bodies (*fd*) presumed to be fat droplets, some glycogen granules, and abundant fibrils (*f*).

Reactive Astrocytes

The nature and severity of the response of astrocytes to ionizing radiation, and the time at which the changes appear, are dependent upon the radiation dose to which the tissue was exposed, and therefore are functions not only of initial surface dose, but also of energy distribution through the cortex (see Fig. 1). The first series of morphological alterations to be described are those which appear to be related to the acute response of the astrocyte to irradiation.

The second series of changes to be considered are those which relate the astrocyte to scar formation. The changes to be described represent the chief pathological events seen in astrocytes in this material. Signs of destruction of astrocytes (12) were never observed, and the number of astrocyte nuclei seen in the lesion zone under light microscopy (Fig. 1 *a*) suggests that the lower doses employed were not lethal for these elements.

THE ACUTE RESPONSE OF ASTROCYTES TO IRRADIATION: All astrocytes in the irradi-

ated portion of the tissue appear to undergo acute changes in response to irradiation. These changes are similar to those seen in focal necrosis months after irradiation. The acute response is therefore probably not specific to irradiated astrocytes, but is representative of astrocytic responses to a variety of noxious stimuli, including direct irradiation, or local tissue degeneration.

In the first 24 hours after exposure to alpha particle irradiation of light and moderate dose, astrocytes of the irradiated portion of the cortex show a marked increase in the number of glycogen granules. This is most prominent in the fine processes scattered through the neuropil and around the small blood vessels (Fig. 8 and 9). Simultaneously, a great increase in the number of mitochondria is encountered in the perinuclear cytoplasm of the cell. The characteristic density of the matrix of mitochondria is preserved (Fig. 6). There is often an increase in the extent of Golgi membrane system, but this is not so striking as the changes in number of mitochondria and glycogen

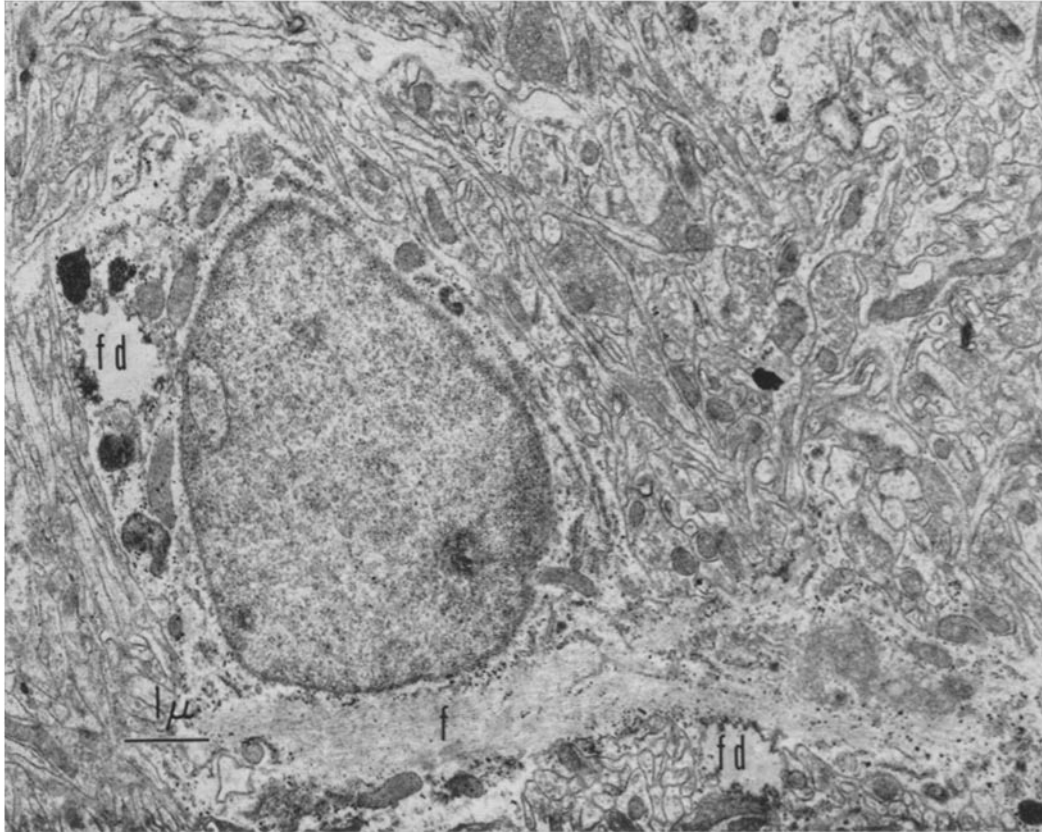


FIGURE 11 Eleven days post irradiation, 6000 rad. Astrocyte of the scar-forming type. This cell contains a liberal sprinkling of glycogen granules, and two fat droplets (*fd*) are still evident. Most prominent in the cytoplasm is the thick bundle of fibrils (*f*) sweeping past the nucleus into a sturdy process.

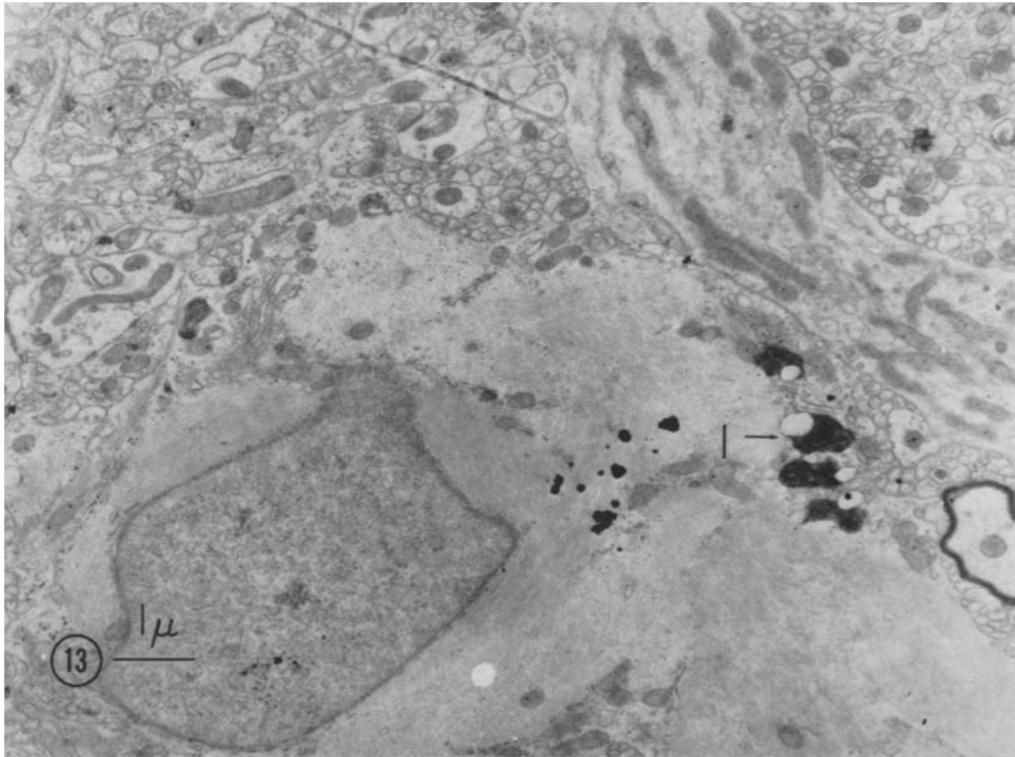
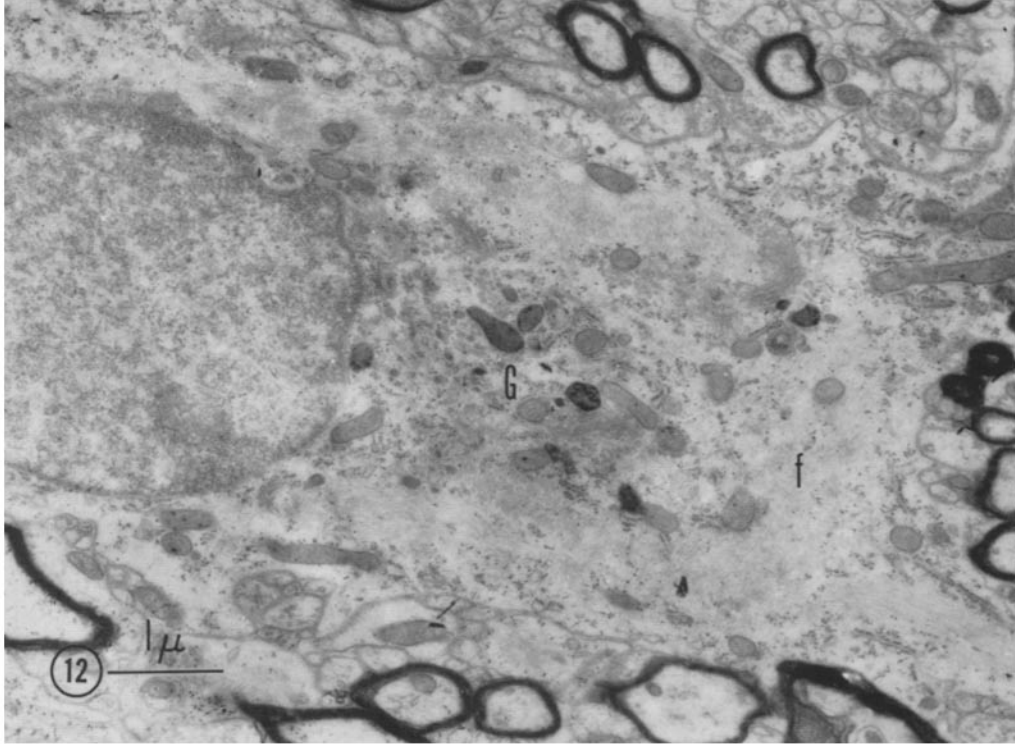
particles. The changes in astrocyte cytoplasm 24 hours after heavy dose irradiation are the same as those after lower dose exposures, except that they anticipate the severity of the response to the lower dose exposures (Fig. 1 *c*). However, 24 to 48 hours after very heavy alpha particle irradiation, no recognizable astrocyte cytoplasm can be found in the necrotic tissue to the end of particle range.

During the first week after irradiation, the

vascular end-feet of astrocytes increase in size (Figs. 8 and 9) and probably in number, and the glycogen content increases. Whorls of membrane, which appear to be reduplications of the plasma membrane (Fig. 9), are often encountered in the vascular end-feet. The perinuclear cytoplasm during this period is also expanded in volume, and contains an abundant and often well organized endoplasmic reticulum.

FIGURE 12 Twenty-two days post irradiation, 20,000 rad. A scar-forming astrocyte beneath the necrotic zone. The nucleus of the cell is at the left. In the center a well developed Golgi zone (*G*) is seen. The dark bodies in this zone may be lysosomes. The remainder of the cytoplasm is filled with the fibrils (*f*) characteristic of this form of astrocyte.

FIGURE 13 Twelve weeks post-irradiation, 9000 rad. Late scar-forming astrocyte. The perinuclear cytoplasm is filled with fibrils. A few dense bodies (*l*) similar to lipofuscin granules are indicated. The small black spots near the center of the figure are a staining artifact.



The increase in glycogen content seems to have reached its peak in most astrocytes at the time when neuronal degeneration is first clearly evident, thus permitting independent localization of the lesion zone. Indeed, this band of glycogen-filled processes represents the most quickly recognized clue for localizing the zone of neuron perikaryon destruction, and is useful in pinpointing the zone of maximum ionization in material sacrificed after shorter postirradiation intervals. Light microscopy of such a zone reveals PAS-positive material (Fig. 1 *c*), but a more intense reaction above and below, as described by Klatzo *et al.* (13), could not be identified in our material.

The nuclei of some acutely reactive astrocytes contain multiple nucleoli. This dispersion of nucleolar material seems suggestive of preparation for division, although no clear evidence for mitotic division of astrocytes could be obtained from our material. The granular nucleoplasm of other reactive astrocytes is commonly aggregated along the nuclear periphery.

Fatty inclusions 1 to 2 μ in diameter may be apparent in the cytoplasm of astrocytes (Fig. 10). These droplets are usually lightly stained, often with a relatively dense peripheral rim, and may be smoothly round or ovoid, but are more often serrated in profile (Fig. 10). At later stages, fat droplets can be found in vascular end-feet. Although fatty inclusions have frequently been interpreted as indicative of phagocytosis in pathological material, there is no evidence of astrocytes ingesting extracellular debris in our material.

SCAR FORMATION: An increase in the amount of the cytoplasmic fibrillar component becomes more evident at later stages. Large fibrillar bundles become prominent in the perinuclear cytoplasm as well as in the roots of the robust processes which are characteristic of astrocytes subsequent to the peak accumulation of glycogen (Figs. 10 and 11). Occasionally, large bundles of fibrils can be seen in the smaller processes, and in vascular end-feet; this is rare in normal cortical astrocytes.

In the fully developed laminar lesion, a scar is readily recognizable by the presence of astrocytes whose cytoplasm is filled with fibrils and displays diminished quantities of glycogen and mitochondria (Figs. 10 to 13). Similar scar-forming astrocytes can be found below the necrotic zone produced with heavy dose irradiation (Fig. 12). The nuclei of the astrocytes in this phase appear

to contain more evenly dispersed chromatin than do those of the acutely reactive form.

For several months after irradiation, occasional processes of astrocytes densely packed with glycogen granules can be found in the neuropil. Such accumulations may reflect a response to local tissue destruction due to delayed radionecrosis, rather than a persisting response of astrocyte cytoplasm to the initial irradiation.

DISCUSSION

The extensive destruction of neurons, nerve fibers, and myelin (14) in the lesion zone in the material of this study is perhaps in some ways comparable to the experimentally induced demyelination studied by Bunge *et al.* (4). These workers were able to identify only a single glial variety in the initial stages of spinal cord demyelination, which they originally identified as "reactive astrocyte" (4), and later termed "reactive macroglia" (3). They believe these latter cells to be derived from oligodendrocytes which invade the demyelinated zone from adjacent normal tissue. They view these cells as having the capacity either to remyelinate the axons, or to differentiate into astrocytes with a markedly increased fibrillar content. This interpretation is difficult to reconcile with the present study, in which there is no indication that macroglia undergo alteration to more primitive forms (*i.e.*, spongioblasts), or that astrocytes ever acquire the characteristics of any other glial elements. The differences in experimental material between the present study and that of Bunge *et al.* (3, 4) may explain some of the conflicting interpretations. The lesion studied by Bunge *et al.* was a demyelinating one only, occurring in a subpial rim of spinal cord, and varied in individual animals. Fixation was obtained by subarachnoid infiltration with osmium tetroxide, and hence their material is not directly comparable with ours.

There can be little doubt that the glial cells whose morphology in normal and reactive states is described in this report are identifiable as the astrocytes of light microscopy. These cells conform in all respects to the generally accepted criteria for identification of astrocytes in electron microscopy (1, 3, 4, 6, 7, 11, 19, 22, 23, 24, 28, 33). The demonstration of glycogen granules throughout the cytoplasm, and their striking accumulation in the acutely reactive state following irradiation, further emphasize the correspondence between the astrocyte of light microscopy and that of

electron microscopy, if the following points are recalled: (a) The astrocyte has long been known by light microscopists to contain glycogen, and to accumulate it in reactive states (9, 31); (b) Klatzo *et al.*, in a histochemical study of the radiation-induced laminar lesion, demonstrated glycogen accumulation in astrocytes as an early response to the irradiation (13); (c) Friede (9) has suggested that the predominantly glycolytic metabolism of the astrocyte, in comparison with other glial elements, is subject to a more prompt and dramatic adaptive change in the reactive state. Additionally, in the present study, (d) it has been possible to demonstrate that the scar-forming astrocyte represents the extreme end of the spectrum of cells which display the glycogen and fibrils characteristic of normal astrocytes. Finally, (e) the subpial astrocyte displays the same cytoplasmic components.

The presence of glycogen granules in many of the processes of normal astrocytes enables the microscopist to appreciate the ample distribution of astrocyte cytoplasm throughout the neuropil of the cerebral cortex. Capillaries, for example, possess nearly complete end-foot investments, so attenuated that they might well be overlooked if the glycogen had not so clearly "labeled" them as astrocyte cytoplasm. Similarly, some of the minute processes which populate the neuropil are beyond the limits of resolution of the light microscope, but may be identified as astrocyte cytoplasm on the basis of the contained glycogen, even in the absence of distinctive fibrils. The extensive distribution of many fine processes is consistent with the configuration of the protoplasmic astrocyte of light microscopy generally found in gray matter.

The demonstration of glycogen in astrocytes seems to depend, in electron microscopy as in light microscopy (32), upon perfusion fixation with an appropriate preservative. The histochemical studies of Friede (9) demonstrated glycolytic pathways in the astrocyte. Three minutes of circulatory arrest before formalin perfusion results in disappearance of astrocyte glycogen (presumably through anaerobic glycolysis) although no other signs of poor fixation are apparent. Immersion in slowly penetrating fixatives such as osmium tetroxide, or fixation by perfusion methods which require extensive washing out of the vascular tree before introduction of the fixative, may permit glycolysis to remove most of the glycogen before the tissue is killed and fixed.

The increase in the amount of glycogen in

astrocytes is the earliest sign of response to irradiation noted in this study, and begins before vascular permeability changes were detected with fluorescein-labeled serum protein by Klatzo *et al.* (13). It seems likely that the shift from glycolytic metabolism to oxidative systems noted by Friede in reactive astrocytes (9) could account for the accumulation of unused substrate. An alternative hypothesis is favored by Klatzo *et al.* (13) for the glycogen accumulation, and is based upon the view that injured tissue liberates glycogen which is taken up by pinocytosis.

Isolated patches of glycogen-filled astrocyte cytoplasm can be seen in the neuropil for at least 6 months after irradiation, probably as a response to delayed focal radionecrosis of neural elements. Indeed, such patches are commonly encountered near degenerating axons, and may well be best explained by the hypothesis of Klatzo *et al.* (13). On the other hand, the accumulation of glycogen occurring immediately after irradiation is very likely a direct effect of irradiation upon the metabolic machinery of the astrocyte, since it occurs before any other sign of tissue injury. It would be premature to attempt to choose between the several reasonable hypotheses for the transient accumulation of glycogen, and for the apparently related accumulation of fat.

The lesion material described here is not directly comparable to cicatrix formation (30) because of the failure of cells to invade from the leptomeninges and blood vessels. The glial "scar" in laminar lesions at long postirradiation intervals is devoid of collagen or other foreign material and apparently consists solely of astrocyte cytoplasm containing an extraordinary increase in number of glial fibrils (16, 23, 30). The number of glial nuclei in the lesion band shown in Fig. 1 *b* does not appear to be markedly increased (or reduced) as compared with that in adjacent normal cortex. It is clear that neuron perikarya are far more susceptible to radionecrosis than are glial elements. With moderate to heavy irradiation doses there appears to be a mild degree of gliosis as judged by an increase in number of astrocyte nuclei at the upper edge of the laminar lesion, but the increase is only slight. A true "scar" can be seen only with high doses of radiation. Heavy dose lesions produce a cavitation and scar containing invading elements, and this material will be presented elsewhere (21).

This work was supported by United States Public Health Service grants B-3604 and B-2684, and Atomic Energy Commission grant AT(11-1)-34 project no. 68. Dr. Maxwell is a John and Mary R. Markle Scholar. We are particularly indebted to Drs. Cornelius A. Tobias and John H. Lawrence for providing accelerator facilities and much helpful advice, to Dr. Harold Richardson and Mr. Thomas Heric for help in the irradiation procedures, and to

Dr. Tor Brustad, Mr. John Lyman, and Mr. David Love for their assistance in dosimetry and in operation of the accelerator. We also gratefully acknowledge the assistance of Miss Sharon Ucker and Mrs. Lillian Berkowitz in the light microscopic preparations and to Mrs. R. Severin and Mrs. Olga Fiorello for their technical assistance in the electron microscopy.

Received for publication, June 29, 1964.

REFERENCES

1. BODIAN, D., An electron-microscopic study of the monkey spinal cord, *Bull. Johns Hopkins Hosp.*, 1964, **114**, 13.
2. BRUSTAD, T., ARIOTTI, P., and LYMAN, J., Experimental setup and dosimetry for investigating biological effects of densely ionizing radiations, *Univ. Calif. Rad. Lab. Repts.*, no. 9454, 1960.
3. BUNGE, M. B., BUNGE, R. P., and RIS, H., Ultrastructural study of remyelination in an experimental lesion in adult cat spinal cord, *J. Biophysic. and Biochem. Cytol.*, 1961, **10**, 67.
4. BUNGE, R. P., BUNGE, M. B., and RIS, H., Electron microscopic study of demyelination in an experimentally induced lesion in adult cat spinal cord, *J. Biophysic. and Biochem. Cytol.*, 1960, **7**, 685.
5. CAJAL, S. RAMÓN Y, *Histologie du système nerveux de l'homme et des vertébrés*, Paris, A. Maloine, 1911.
6. COULTER, H. D., Electron microscopic identification of glial cells in the central nervous system of adult mice and rats after perfusion fixation, *Anat. Rec.*, 1964, **148**, 273.
7. FARQUHAR, M., and HARTMANN, J., Neuroglial structure and relationships as revealed by electron microscopy, *J. Neuropath. and Exp. Neurol.*, 1957, **16**, 18.
8. FLEISCHAUER, K., Über die Feinstruktur der Faserglia, *Z. Zellforsch.*, 1958, **47**, 548.
9. FRIEDE, R. L., The cytochemistry of normal and reactive astrocytes, *J. Neuropath. and Exp. Neurol.*, 1962, **21**, 471.
10. GRAY, E. G., Electron microscopy of neuroglial fibrils of the cerebral cortex, *J. Biophysic. and Biochem. Cytol.*, 1959, **6**, 121.
11. HARTMANN, J. F., Two views concerning criteria for identification of neuroglia cell types in electron microscopy. Part A, in *Biology of Neuroglia*, (W. F. Windle, editor), Springfield, Ill., Charles C Thomas, 1958, p. 50.
12. JANSSEN, P., KLATZO, I., MIGUEL, J., BRUSTAD, T., BEHAR, A., HAYMAKER, W., LYMAN, J., HENRY, J., and TOBIAS, C., Pathologic changes in the brain from exposure to alpha particles from a 60-inch cyclotron, in *Response of the Nervous System to Ionizing Radiation*, (T. J. Haley and R. A. Snider, editors), New York, Academic Press, Inc., 1962, p. 382.
13. KLATZO, I., MIGUEL, J., TOBIAS, C., and HAYMAKER, W., Effects of alpha-particle radiation on the rat brain, including vascular permeability and glycogen studies, *J. Neuropath. and Exp. Neurol.*, 1961, **20**, 459.
14. KRUGER, L., and CLEMENTE, C. D., Anatomical and functional studies of the cerebral cortex by means of laminar destruction with ionizing radiation, in *Second International Symposium on the Effects of Ionizing Radiation on the Nervous System*, (T. Haley, editor), Boston, Mass., Little, Brown and Co., 1964, p. 84.
15. LUFT, J. H., Improvements in epoxy resin embedding methods, *J. Biophysic. and Biochem. Cytol.*, 1961, **9**, 409.
16. LUSE, S. L., The ultrastructure of normal and reactive astrocytes, *Lab. Invest.*, 1958, **7**, 401.
17. LUSE, S. L., Ultrastructure of the brain and its relation to transport of metabolites, *Res. Publ. Assoc. Res. Nervous and Mental Disease*, 1962, **40**, 1.
18. MALIS, L. I., BAKER, C. P., KRUGER, L., and ROSE, J. E., Effects of heavy ionizing, monoenergetic particles on the cerebral cortex. I. Production of laminar lesions and dosimetric considerations, *J. Comp. Neurol.*, 1960, **115**, 219.
19. MAXWELL, D. S., and KRUGER, L., Electron microscopy of normal and reactive astrocytes in rat cerebral cortex, *Anat. Rec.*, 1964, **145**, 310.
20. MAXWELL, D. S., and KRUGER, L., Electron microscopy of radiation induced laminar lesions in the cerebral cortex of the rat, in *Second International Symposium on the Effects of Ionizing Radiation on the Nervous System*, (T. Haley, editor), Boston Mass., Little, Brown and Co., 1964, p. 54.
21. MAXWELL, D. S., and KRUGER, L., small blood vessels and the origin of phagocytes in the rat cerebral cortex following heavy particle ir-

- radiation as studied with the electron microscope, *Exptl. Neurol.*, 1965 (in press).
22. MAYNARD, E. A., SCHULTZ, R. L., and PEASE, D. C., Electron microscopy of the vascular bed of rat cerebral cortex, *Am. J. Anat.*, 1957, **100**, 409.
 23. PALAY, S. L., An electron microscopical study of neuroglia, in *Biology of Neuroglia*, (W. Windle, editor), Springfield, Ill., Charles C Thomas, 1958, p. 24.
 24. PALAY, S. L., MCGEE-RUSSELL, S. M., SPENCER, G., JR., and GRILLO, M. A., Fixation of neural tissues for electron microscopy by perfusion with solutions of osmium tetroxide, *J. Cell Biol.*, 1962, **12**, 385.
 25. PEASE, D. C., Buffered formaldehyde as a killing agent and primary fixative for electron microscopy, *Anat. Rec.*, 1962, **142**, 342.
 26. REVEL, J. P., NAPOLITANO, L., and FAWCETT, D. W., Identification of glycogen in electron micrographs of thin tissue sections, *J. Biophysic. and Biochem. Cytol.*, 1960, **8**, 575.
 27. REYNOLDS, E. S., The use of lead citrate at high pH as an electron-opaque stain in electron microscopy, *J. Cell. Biol.*, 1963, **17**, 208.
 28. SCHULTZ, R. L., Macroglial identification in electron micrographs, *J. Comp. Neurol.*, 1964, **122**, 281.
 29. SCHULTZ, R. L., MAYNARD, E. A., and PEASE, D. C., Electron microscopy of neurons and neuroglia of cerebral cortex and corpus callosum, *Am. J. Anat.*, 1957, **100**, 369.
 30. SCHULTZ, R. L., and PEASE, D. C., Cicatrix formation in rat cerebral cortex as revealed by electron microscopy, *Am. J. Path.*, 1959, **35**, 1017.
 31. SHIMIZU, N., and HAMURO, Y., Deposition of glycogen and changes in some enzymes in brain wounds, *Nature*, 1958, **181**, 781.
 32. SHIMIZU, N., and KUMAMOTO, T., Histochemical studies on the glycogen of the mammalian brain, *Anat. Rec.*, 1952, **114**, 479.
 33. TERRY, R. D., and WEISS, M., Studies in Tay-Sachs disease. II. Ultrastructure of the cerebrum, *J. Neuropath. and Exp. Neurol.*, 1963, **22**, 18.
 34. VOGEL, F. A., and KEMPER, L., Modifications of Hortege's silver impregnation methods to assist in the identification of neuroglia with electron microscopy, *Proc. IV Internat. Congr. Neuropath.*, 1961, **2**, 66.
 35. WATSON, M. L., Staining of tissue sections for electron microscopy with heavy metals. II. Application of solutions containing lead and barium, *J. Biophysic. and Biochem. Cytol.*, 1958, **4**, 727.